Chapter

High Power Very Low Voltage Electric Motor for Electric Vehicle

Daniel Matt, Nadhem Boubaker, Mourad Aitakkache, Philippe Enrici, Jean-Jacques Huselstein and Thierry Martire

Abstract

Electric vehicles are often designed in the same way as their conventional counterparts based on the internal combustion engine, they are heavy machines for comfort and safety reasons, and increasingly powerful. Under these conditions, in order to simplify the motor electrical supply system by reducing the current levels, the voltage chosen for the battery is very high and can go up to 700 V. However, for many applications where the power is relatively low (< 30 kW per motor), it can be more beneficial to size the system at very low voltage (< 60 V). This approach allows to overcome many constraining safety requirements and also to use off-the-shelf components (motor controllers, connectors, etc.) that are more easily available on the market in this voltage range. There are also many regulatory provisions that may require to stay within this voltage limit. This article presents a variety of very low voltage motorisation solutions with a required power up to 100kW. They use two complementary approaches. The first is to implement an original permanent magnet synchronous machine technology with an optimised armature winding for low voltage operation. The second is based on power splitting where the electrical machine being designed to be driven by multiple controllers. Many examples of low-voltage motorised vehicles (sporty vehicle, tractor, re-motorised automobile, etc.) are illustrated in this article.

Keywords: Electric Vehicle, Very Low Voltage, Synchronous Machine, Permanent Magnet, Solid Bar Winding, Power Splitting

1. Introduction

For the sake of safety, the standards and regulations limit the supply voltage level for the electric vehicles drive system. The standards dealing with the very low voltage systems (VLV) provide a general guidance. For example, the 2014/35/UE European Directive for the CE marking fixes the voltage level at 75 V DC, hence, in practice this could be the choice for the battery voltage.

Furthermore, in the automotive realm, the European Regulation R100 concerning the approval of vehicles with regard to specific requirements for the electric powertrain, has even reduced the maximum voltage level to 60 V (Class A). This range of voltage will therefore ease the design constraints and the operational maintenance of the vehicle. The 60 V is generally considered as the reference level of VLV for electric vehicles.

At this low voltage range, there is a large choice of commercially available off-the-shelf components for the power electronics needed to drive the electric motor, regardless its technology, DC motor, synchronous motor or induction motor, though knowing that the permanent magnet synchronous motors are emerging as one of the best candidate to dominate the market of powertrain electrification.

However, at low voltage, when the level of the required electrical power reaches a certain threshold, which is around 30 kW, the availability of the power electronics components becomes considerably limited given the high current level to be handled by the controller, which is greater than 500A at a battery voltage of 60 V. Indeed, this poses very challenging constraints on the design of the power modules where the high current gets closer to the switching capability limit of the transistors available on the market (very low voltage MOS technology). We will be detailing the challenges and the associated solutions related to this topic in a later section of the chapter.

The technology outlined in this chapter, where many validation prototypes are presented, brings some original solutions to the design of very low voltage electric powertrains, even at high power level. Many electric vehicles presented in this chapter involving a power as high as 100 kW.

First of all, we will discuss the design techniques of an electric motor being optimised to operate at very low voltage. Afterwards, several techniques of power distribution have been described, which enables the required total electrical power to be shared between several controllers. Finally, we present an overview of the limits of feasibility of the power electronics that would be required to drive electric motors at very low voltage, based on the current available technologies of the semiconductors components.

2. Very low voltage electric motor

2.1 Solid bar winding

When an electric motor is operating at very low voltage, there is an opportunity to optimise its winding in order to significantly enhance its performance. Conventionally, the windings of electric motors are based on an enamelled round wire (loose random conductors), as illustrated in the **Figure 1b**. In this case, the copper

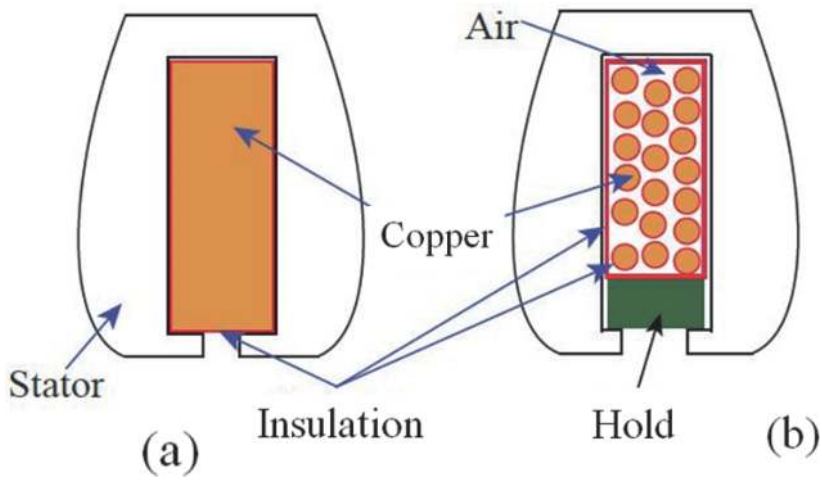

Figure 1.
(a) Solid bar winding vs. (b) Round wire winding.

fill factor inside the stator slot is very poor, where, unless relying on non-conventional manufacturing processes (segmentation, etc.), only around 40% can be achieved in the best case (pure copper CSA/naked slot area), it can be even less than 30% when considering very small size motors with tiny slots.

At very low voltage, the conductors inside the slot are connected in parallel where the number of turns is inherently very low. In the case of a winding design with one turn per slot, which is often the case at VLV, it appears to be more judicious to replace the multi-strand conductor with a single solid copper bar adjusted to the slot dimensions, as illustrated in the **Figure 1a**. In the latter case, the copper fill factor inside the slot can reach approximately 80%, which consequently doubles, even triples, the copper volume for a given motor size.

At a constant copper loss and a given slot cross sectional area, the relationship between the RMS current, I_b, in the solid bar conductor and the total RMS current, I_f, in the equivalent slot wound with multi-strand round conductor is as follows:

$$I_b = I_f.(\sigma_{rb}/\sigma_{rf})^{1/2} \quad (1)$$

The coefficients σ_{rb} and σ_{rf} represent the copper fill factor inside the slot with solid bar conductor and with multi-strand round conductor, respectively. With the 80% fill factor in the first case and 35% in the second one, the current carried by the solid bar conductor is 50% higher, and, consequently, the output torque of the motor increases in the same proportion.

The **Figure 2** illustrates how difficult it is to perform a high quality winding with loose round wire. It can be easily noticed that a non-negligible part of the copper is located outside the active part of the motor (i.e. stator). This bulky copper outside the stator slots increases the volume, the weight and the loss of the machine. All these drawbacks are addressed with the use of a solid bar conductor.

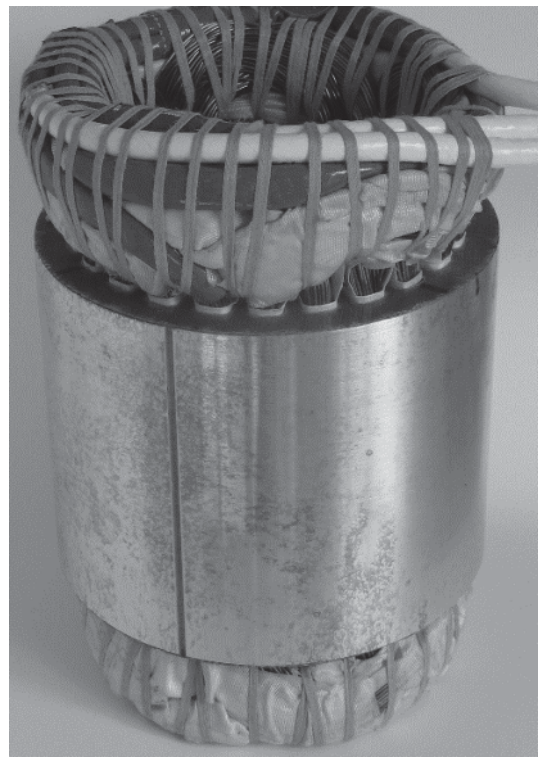

Figure 2.
Electric motor end-windings wound with loose round wires.

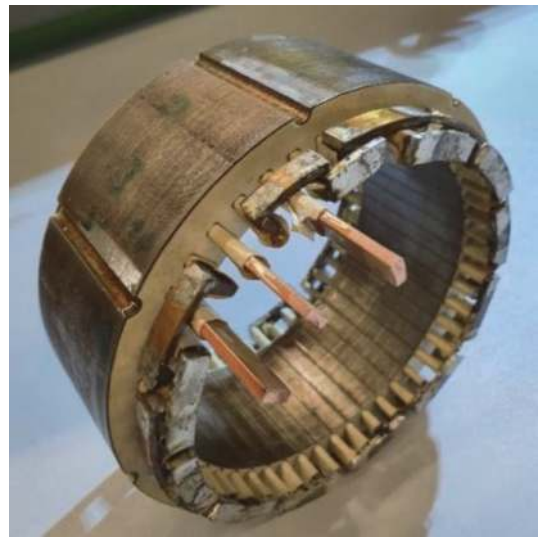

Figure 3.
Solid bar winding, distributed winding.

Figure 4.
Solid bar winding, wave concentrated winding.

Figures 3 and **4** illustrate some of our products made using a solid bar winding. It can be easily seen that the useless copper at the end-windings (overshooting the stator core pack) is less bulky and well controlled. These proposed winding techniques are most convenient for low voltage electrical machines.

The distributed winding shown in **Figure 3**, with one slot per pole and per phase, is well suited to medium range power machines (a few tens of kW) operating at few hundreds Hz electric frequency [1–3]. The structure shown in **Figure 4** is more original where the phases are wound around the tooth (wave concentered winding) and grouped in separate sectors [1, 4, 5], without phase overlaps at the end-windings of the machine. This structure is rather well suited for small electrical machines which can then operate at very high frequency (up to 2000 Hz), the resulting winding is very compact.

This technique is not commonly used in practice due to the fact that the solid bars are prone to very high AC copper loss (under alternating regime) which can be much higher than the DC ohmic loss.

Additional losses in massive conductors can be prohibitive, but a detailed study of these phenomena [1, 4] shows that the advantages of the approach largely outweigh the disadvantages if the winding is appropriately designed [1, 3, 4].

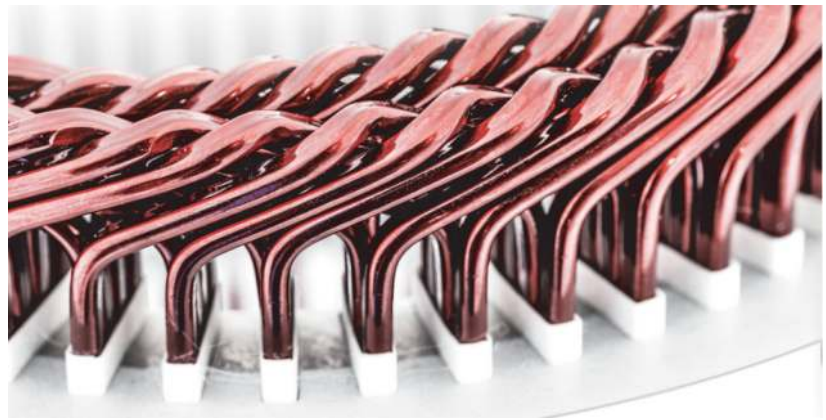

Figure 5.
Hairpin winding (courtesy of special machine tool company).

Paradoxically, the concept can be perfectly applied, as we will see, to high pole count electric motors operating at high frequency, which is the case for all machines with high power density for embedded applications.

Many industrial motor manufacturers, especially for electric vehicles, are using the solid bar copper winding, in particular via the "hairpin" technique consisting in a "pin" forming that can ease the overlapping of conductors at the end-windings (cf. **Figure 5**), but the overall design approach of these machines remains conventional, especially because it uses several conductors per slot. The approach presented in this chapter is distinguished by the use of a single solid bar per slot (one turn per slot), which allows to optimise many parameters and to reach unmatched level of compactness, for high power electric motors operating at very low voltage.

In summary, the main pros in using solid bars are:

- Enhanced copper fill factor (80% filling instead of 40%).
- The iron-copper thermal resistance is reduced.
- The slots opening width can be very small which increases the flux density in the air gap and decreases the cogging torque and eventually the torque ripple.
- The copper overhangs are very compact and controlled.
- The winding manufacturing process is simplified and can be easily automated.
- The machine is more robust and reliable.

And the main cons are:

- Higher copper loss density
- The connection of the copper bars in order to form the whole winding is more complex.

2.2 Additional losses in the solid copper bars

In order to be able to effectively implement the technique of winding with single bar per slot, it is mandatory to fully control the additional copper losses associated with the operation at high electrical frequency.

The different phenomena related to alternating flux density inside the copper yielding to excessive loss are well describes in the literature [6, 7], however we recall here the two main ones.

In order to quantify the loss increase, the k_{AC} coefficient is introduced, which is the ratio of the total AC copper loss, P_{AC}, to the DC copper loss, P_{DC}, in the winding, at given current:

$$k_{AC} = P_{AC}/P_{DC} \tag{2}$$

The best known phenomenon causing these additional losses is called "skin effect", it appears in any electrical conductor carrying an alternating current. The skin effect tends to push the current back to the periphery of the conductor, as shown in the following **Figure 6**.

The current density, J, in a round conductor, as a function of the distance from the periphery, r, in sinusoidal regime, is expressed by the following relationship:

$$J(r) = J_0 . e^{-\frac{r}{\delta}} . \cos\left(\omega t - \frac{r}{\delta}\right) \tag{3}$$

where δ represents the skin depth at a conductivity σ of the conductor:

$$\delta = \frac{1}{\sqrt{\sigma \mu_r \mu_0 \pi f}} \tag{4}$$

The current density at the skin depth is roughly equal to 37% of its value at the surface, while it is only equal to 5% at three times δ.

In the case of a rectangular conductor the relationships of the skin effect are more complex. The following equation [1, 6] is valid for both cases round conductor and rectangular conductor, and allows to precisely quantify the increase in copper loss due to the skin effect:

$$K_{AC} = \sqrt[6]{\left(\frac{3}{4}\right)^6 + \left(\frac{S}{p\delta}\right)^6} + \frac{1}{4} \tag{5}$$

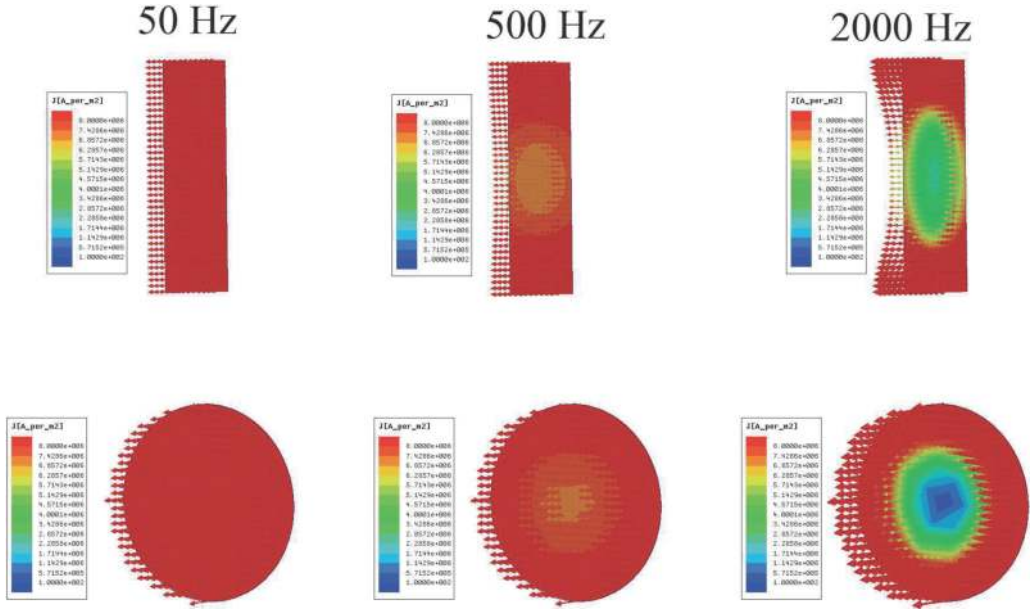

Figure 6.
Current density distribution in two conductors having the same cross-section with round and rectangular shape at different frequencies [1].

S and p respectively represent the cross section area and the perimeter of the conductor.

Table 1 gives the values of K_{AC} for different bar shapes (used in the prototypes presented later) and different frequencies. The dimensions of the bar are defined in **Figure 7**.

According to the **Table 1**, in the worst case scenario, the increase in copper loss due to the skin effect is less than 1%, so this phenomenon is not significant at the considered frequencies.

The second observed phenomenon causing excess copper loss is known as field effect or inductance effect. Unlike the skin effect, it only takes place in the copper volume surrounded by a magnetic circuit (stator). This phenomenon is depicted in **Figure 8**. In this case, the additional loss is due to the transverse flux (slot leakage flux) produced by the armature current, which closes in the slot width (t_{enc}), creating induced currents in the solid bar which will lead to an uneven current density distribution, being much higher in the lower part (near the slot opening) than in the upper part of the solid bar.

The field effect phenomenon is the main cause of increased losses, where the K_{AC} coefficient can be greater than 4 if it is not well controlled, which would cancel out most of the benefits introduced by the use of the solid bar winding.

The coefficient K_{AC} related the field can be precisely calculated using the following analytical relationship [1, 7]:

$$k_{AC} = \frac{h_{bar}}{\delta}\sqrt{\frac{t_{bar}}{t_{enc}}} \tag{6}$$

#	Dimensions h_{bar} x t_{bar} (mm)	Frequency (Hz)	δ (mm) à 100 °C	K_{AC}
1	4x5	800	2,7	1,003
2	3x5	1666	1,9	1,009
3	8x4	800	2,7	1,009
4	8x3	133	6,6	1

Table 1.
Skin effect for different copper bar dimensions.

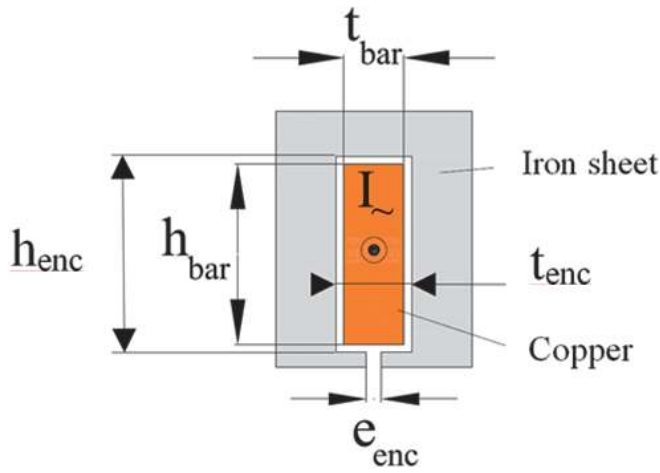

Figure 7.
Main dimensions of the slot and the copper conductor.

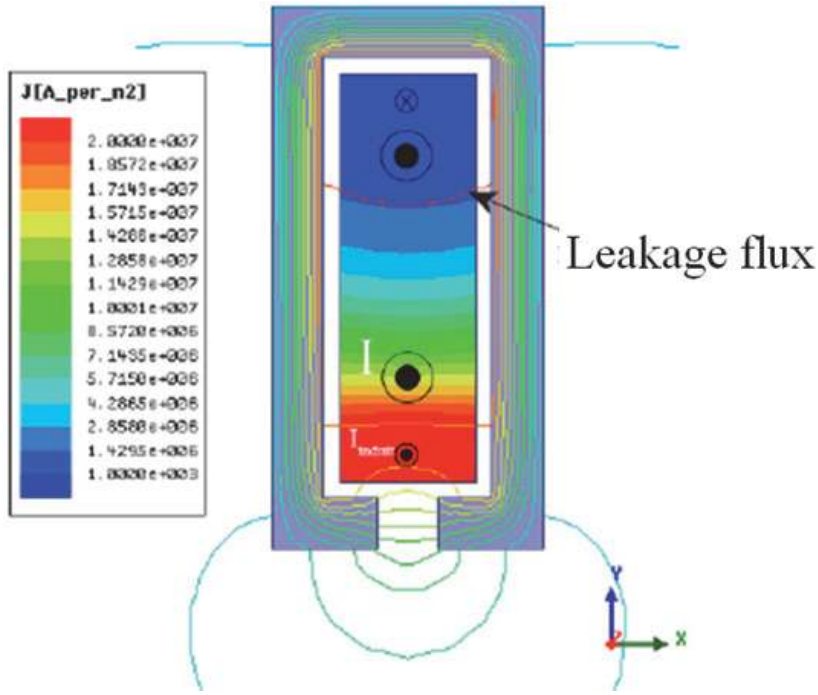

Figure 8.
Illustration of the uneven distribution of the current density inside the conductor due to the slot transverse flux.

#	h_{bar} (mm)	t_{bar}/t_{enc}	Frequency (Hz)	δ (mm) à 100°C	K_{AC}
1	4	0,83	800	2,7	1,35
2	3	0,83	1666	1,9	1,44
3	8	0,8	800	2,7	2,65
4	8	0,75	133	6,6	1,05

Table 2.
Field effect for different copper bar dimensions.

This relationship is only valid when $K_{AC} > 1$. **Table 2** summarises the value of K_{AC} for exactly the same configurations considered in **Table 1**.

According to the results presented in **Table 2**, it can been clearly seen that, as expected, the increase in copper loss due to the use of solid bars is significant, however, the solid bar still beneficial even at high frequencies when considering the overall performance of the machine. Indeed, in order to illustrate this point, we can consider the configuration # 2 operating at a nominal frequency of 1666 Hz. The use of a solid bar would increase the current in the slot, at constant DC losses, by about 50% (cf. relation (1)), while the increase in losses in AC mode would require it to be reduced by 20% ($\sqrt{1,44}$), hence, the overall increase in torque and current is equal to 25%.

The remaining examples of **Table 2** will be analysed when their corresponding products are presented later in this chapter.

3. Low voltage power electronics converter

3.1 Power converter for electric vehicle

In electric vehicles, the electric motors can be fed by one or more power converters depending on one or multiple energy sources. Whether it is an airplane, an

electric vehicle or a boat, several energy sources are available with different characteristics, operating modes and architectures. The most characteristic quantities are the voltage and the current levels requiring the use of specific power and passive components. The architecture design of these converters, whether forward, isolated or segmented, is a first issue that must be specific to the application. Another problem is the integration of static converters in order to increase their compactness (power-to-weight and power-to-volume ratios) because the high power and the low voltage imply very high currents which are not very favourable to a high efficiency and to a volume reduction. Of course, cost constraints are very important in the automotive field and must be integrated from the start of the design process.

The complex power conversion and management functions implemented in the vehicle concern the electric motor, its control electronics, the transmission and management of energy by the charger and the converters used to power the navigation and entertainment systems. All these elements are supplied with very low voltages ranging from 12 V to 48 V, sometimes 60 V, which leads to favouring the use of 100 V components. At the drive train level, it is recommended to stay at low voltage, in order to simplify the control and most important to optimise the efficiency and therefore enhance the autonomy by avoid putting converters in series to adapt the voltage levels (for example, low-voltage battery and high-voltage motor). In other words, it is better to avoid a DC/DC stage between the battery and the inverter and therefore to only have the inverter between the battery and the motor. Furthermore, in order to recover the energy during braking phases, the DC/DC converter has to be reversible which would make its design more complex.
A classical architecture is given in **Figure 9**.

The electrical connection must also be appropriately designed because for a small vehicle, whether it is full electric or micro/mild hybrid type, with for example a power of around 30 kW at 48 V the currents are very high (650A for 48 V). The wiring with a large cross section must therefore be as short as possible and the inverter placed as close as possible to the motor and the battery, ideally in the same compartment and taking advantage of the car structure to dissipate the heat rejection.

Increasing the power of the electric motor quickly becomes a problem if the supply voltage does not increase proportionally because high DC bus and phase currents lead to an unreasonable increase in the number of semiconductor and passive components required. To reach the required switching capability, the surface area of the PCB, the volume of the cooling system and the size of the connectors should be increased accordingly, thus resulting in a weight increase of the

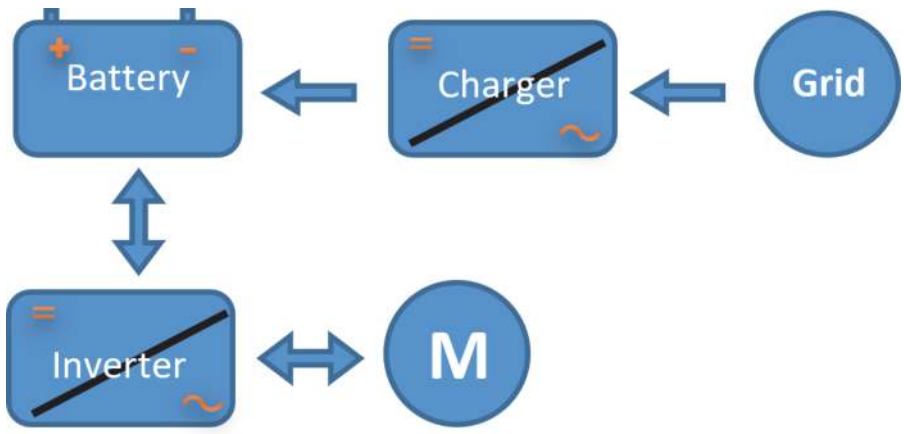

Figure 9.
Example of a drive train with a single power inverter.

electronic system and also a high cost incompatible with the requirements of the automotive field.

Alternatively, when the power becomes too high (at VLV) and therefore the currents are very high (>500A), the solution would be to segment the machine winding into many stars and supply them with several synchronised inverters as shown in **Figure 10**.

In **Figure 10**, the power is shared between two inverters, which mean that there are not too many components in parallel in each inverter arm, and that the inverters are less complex, less cumbersome and easier to build, and, also, that the connections are less bulky with less losses.

3.2 Power components for low-voltage converters

The static converters contains power modules which allow the classical energy conversion functions (AC/DC or DC/AC) and which are generally designed based on two main categories of components, namely the MOSFETs (Metal Oxide Semiconductor Field Effect Transistor) for low voltage inverters or IGBTs (Insulated Gate Bipolar Transistor) for high voltage ones. The field of application and the necessary integration of this static converter make it possible to determine the most suitable components according to several parameters such as power and voltage as well as the switching frequency. **Figure 11** gives a detailed breakdown of the use of these components.

For electric vehicles, the silicon MOSFETs and IGBTs are mainly used. In this field, the battery DC voltage is switched at frequencies ranging from 5 to 20kHz. This switching level is usually achieved by the use of well-adapted control laws. The components required for the DC/AC conversion function are usually packaged in modules. The electric motor of a power train system is three-phase, this implies that the inverter structure must be composed of at least six switches that are bidirectional in current formed by the association of an IGBT with a freewheeling diode or MOSFET in parallel that are naturally bidirectional in current due to their intrinsic integrated diode.

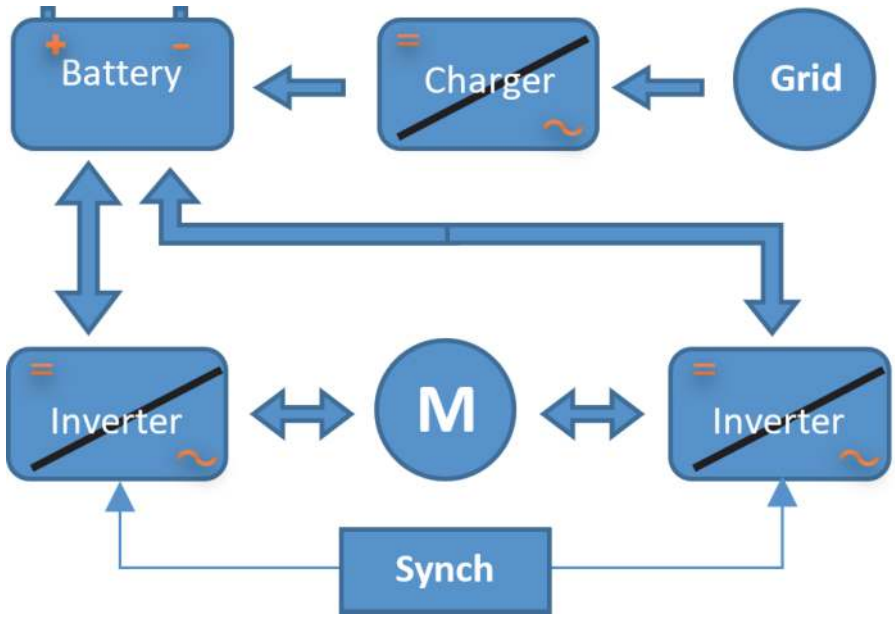

Figure 10.
Distributed system for segmented winding.

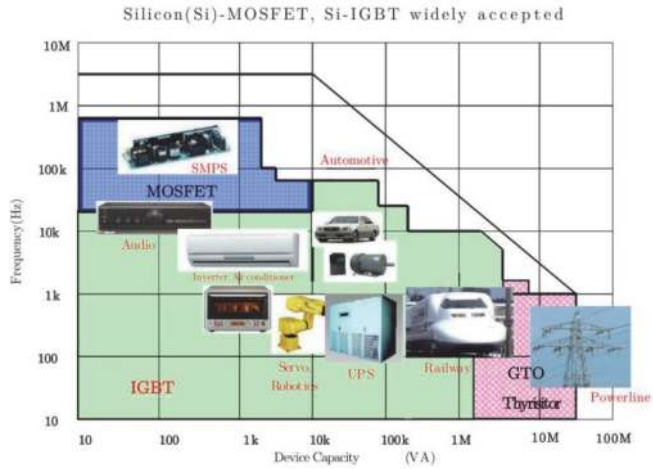

Figure 11.
Use of the different types of switchers depending on the application [8].

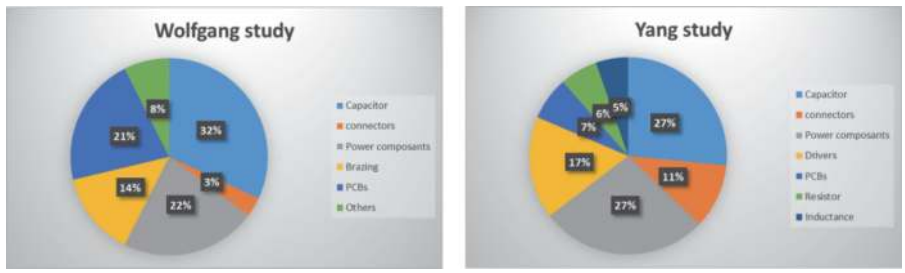

Figure 12.
Distribution of failure sources in a power converter [9, 10].

It is also useful to keep in mind that failures can be experienced in a power converter, it is essential that the reliability of this power converter is as high as possible in the case of an electric vehicle for the obvious safety reasons. Several studies show that the power modules can be the most weak part of a converter [9, 10]. The causes of failure are mainly due to temperature (frequent thermal cycling of components and high steady state current), but also to moisture, vibrations and contaminations during the manufacturing process. The **Figure 12** shows the results of two studies carried out on the failure modes of power converters.

The choice of a very low voltage supply, in this case 60 V, allows the use of commercial converters. However, as soon as the required power imposes a current higher than 500 A, it is necessary to design a bespoke power converter or, alternatively, to associate several of them in parallel. The technological constraints and standardisation lead to given silicon chip sizes which are then the building blocks of larger components. The increase in current capacity is thus achieved by combining elementary units in parallel.

Figure 13 shows some examples of power modules used in some conventional electrified vehicles.

We can note here that the semiconductors are associated in parallel in order to be able to switch important currents which depends on the power and the supply voltage of the machine and thus on the range of the EV (low range, high range, commercial vehicle...).

For example, the Tesla Model S has 10 IGBT chips per phase (i.e. 30 per module) to provide the 800 kW needed to power this vehicle whereas a Renault Zoé only needs 12 IGBT chips per module to ensure its nominal operation at 400 V/300 A.

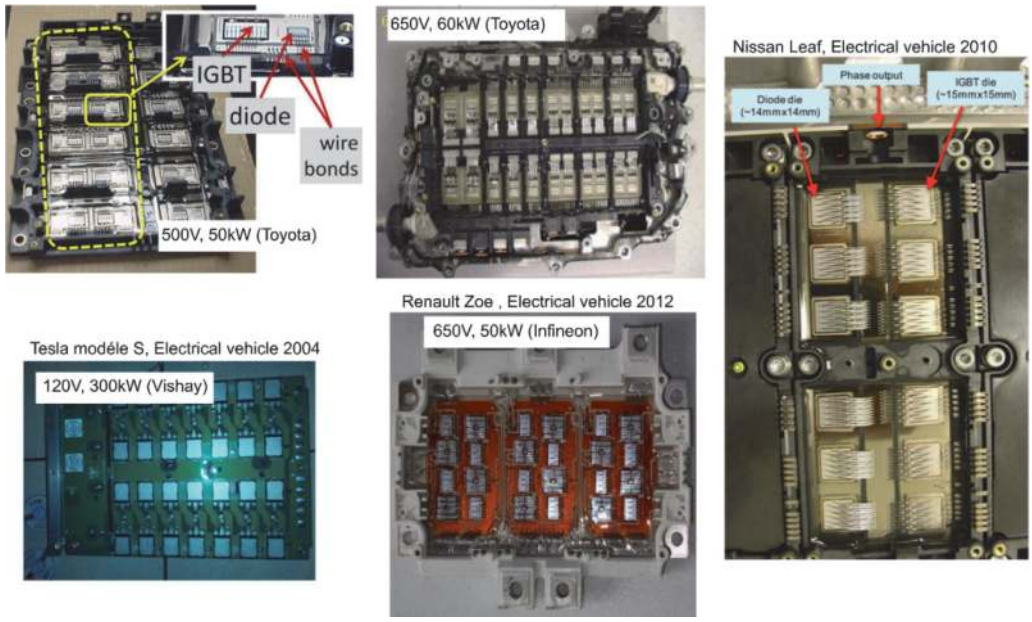

Figure 13.
Examples of inverters in the realm of electric vehicles [11, 12].

The inverter should be compactly designed and should preferably be mounted as close as possible to the motor. The elements that contribute to the performance of the power module and therefore of the inverter are:

- well-balanced current in the parallel MOSFETs,
- low V_{DS} peak at turn-off,
- low R_{dson} when the MOSFETs are turned on,
- low R_{th} of the heat sink.

In addition to conduction losses, switching losses must also be minimised to ensure optimum efficiency and minimal impact on the vehicle autonomy.

The design of the converter must also take into account the control boards, the drivers and the cooling system. **Figure 14** shows the controller and driver circuitry for the Lexus hybrid vehicle.

Nowadays, new materials are emerging to replace silicon such as: silicon carbide (SiC) and Galium nitride (GaN). These materials allow higher switching

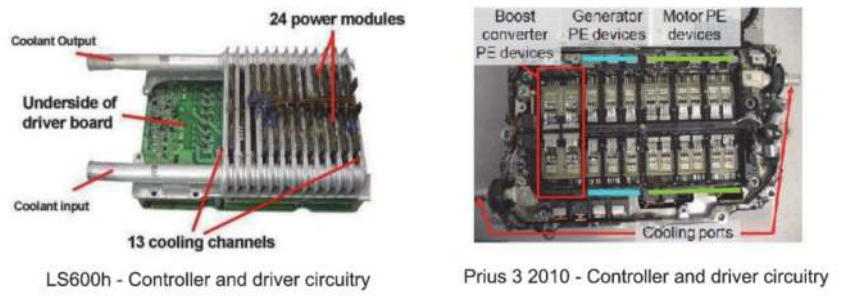

Figure 14.
Examples of controllers and driver circuitry [13].

frequencies, greatly reduced losses and higher operating temperatures resulting in more compact cooling systems, however, they also require a better control of the EMC and the PCB routing.

4. Very low voltage and medium power motorisation for electric vehicles

Many small electric vehicles (boat, kart, motorcycle, quad, cart, utility tricycle, small urban vehicle, unlicensed vehicle…) are equipped with an electrical motorisation with a power ranging from 10 kW to 30 kW. We present in this section a motor architecture optimised to operate at this power level and at very low voltage.

The winding technique for the electric motor is depicted in **Figures 3** and **15**, the slot copper bars are connected to each other at the end-windings via bridges bars located in two planes (crook bar and bow bar). In this case the overhangs are extremely compact. This configuration of the bars corresponds to the case number 1 in **Tables 1** and **2**.

To optimise the manufacturing costs, all motors in this power range will use the same stator laminations, the same number of poles; hence, the number of bars is always the same, only the length of the stator stack is likely to evolve in order to comply with the different specifications, we will be giving two examples.

The motors are assembled in square shaped housing (212x212 mm^2 CSA), as shown in **Figure 16**.

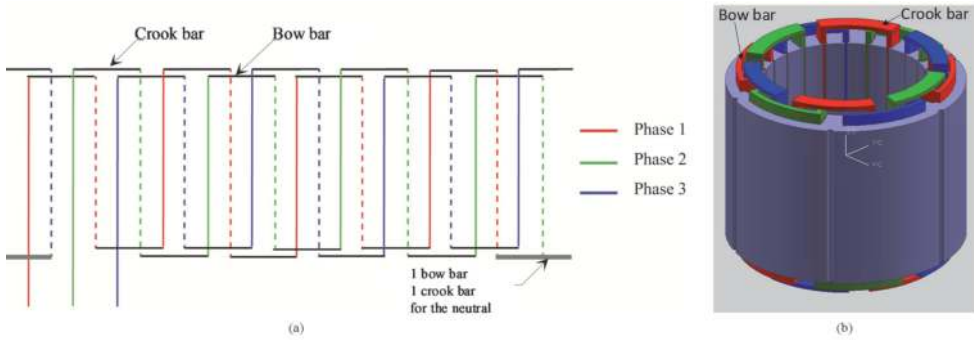

Figure 15.
Winding architecture - 20 kW very low voltage motor. (a) Winding layout, (b) 3D CAD view of the wound stator.

Figure 16.
A motor portfolio with a power ranging from 10 kW to 30 kW, operating at very low voltage (courtesy of SMVE performance SAS).

4.1 Outboard electric motor

The first specification we present is related to a marine outboard motor (electric boat), where the nominal speed of the propeller is 1750 rpm, with a reduction ratio of the transmission angle equal to 2.

The simplified specifications of the motor are as follows:

- Rated power: 10 kW
- Nominal speed: 3500 rpm
- Power supply voltage: 50 VDC
- Efficiency: greater than 90%

There is no need here to detail the EMAG sizing of the motor, which is conventional and does not fit the main purpose of this chapter. The following **Table 3** summarises all the main characteristics of the motor.

This first case of sizing shows that even with a relatively low nominal operating speed, it is possible to reach high specific performances where, in particular, the

Dimensions	
Stator outer diameter	208 mm
Stator inner diameter	172 mm
Magnetic airgap length	1,5 mm
Magnet height	6 mm
Stator stack length	35 mm
Winding bar dimensions (hxw)	4x5 mm
Slot dimensions (hxw)	4,8x5,8 mm
Materials	
Stator corepack	M270-35A
Magnets	N35UH
Electrical parameters	
Pole number	16
Slot number	48
Phase rated current	240A RMS
Phase resistance (AC, K_{AC} = 1,05), 20°C - 100°C	1,3 mΩ - 1,7 mΩ
Torque coefficient kt	0,113 Nm/A
Total weight (including mechanics)	8 kg
Nominal torque-to-weight ratio	3.3 Nm/kg
Joule losses (at 100°C)	300 W
Iron losses + mechanical losses	250 W
Efficiency	95%
Cooling method	Natural convection

Table 3.
Characteristics of the electric boat motor.

power density is higher than 1 kW/kg, without impairing the efficiency. The latter is a key performance in the case of electric boat where the nominal speed corresponds to a permanent operating speed because the vehicle regime is stable during the navigation.

4.2 Kart electric motor

For this second studied case, we use the same motor structure, but considering a much higher power, adapted to the motorisation of a small sport vehicle, a kart for example.

The simplified specifications of the motor are as follows:

- Maximum power: 25 kW
- Maximum speed: 6000 rpm
- Power supply voltage: 60 VDC
- Efficiency: greater than 90%

The following **Table 4** summarises the characteristics of the motor designed for this specification. The laminations are identical to those of the previous case (electric boat Section 4.1).

This sizing case is extreme, because, given the power, we are at the limit of feasibility at VLV, especially if we consider the phase current reaching 500 A. However, contrary to the previous case, the maximum power is transient because the speed of a small sport car is very variable on a winding track, the thermal steady state depends on the nature of the latter.

Even though the efficiency remains good, the losses at maximum power are high, more than 2 kW, but in this vehicle the motor is located outside and will be naturally cooled by a large amount of air flow (**Figure 17**). The maximum speed of the vehicle

Dimensions	
Stator stack length	28 mm
Electrical parameters	
Pole number	16
Slot number	48
Phase rated current	490A RMS
Phase resistance (AC, K_{AC} = 1,35), 20°C - 100°C	1,3 mΩ - 1,7 mΩ
Torque coefficient kt	0,082 Nm/A
Total weight (including mechanics)	7 kg
Nominal torque-to-weight ratio	5,7 Nm/kg
Joule losses (at 100 °C)	1220W
Iron losses + mechanical losses	500 W
Efficiency	94%
Cooling method	Natural convection

Table 4.
Characteristics of the electric kart motor.

Figure 17.
Electric kart.

is well above 100 km/h, a natural convection cooling is sufficient. Furthermore, the heat exchange is improved by the very low copper to iron thermal resistance.

5. High frequency motor for electric airplane

This application illustrates the implementation of the concept for a motor operating at very high electrical frequency for an aeronautical application. It is a laboratory study [1] based on the motorisation specification of one of the first industrial all-electric aircraft, namely the Efan, from AIRBUS (**Figure 18**). The project was

Figure 18.
Prototype Efan (courtesy of AIRBUS).

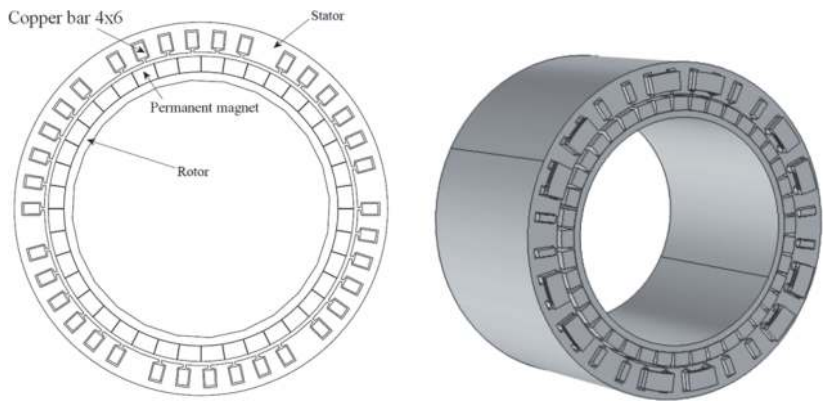

Figure 19.
Structure of the "per group" winding.

quickly abandoned by AIRBUS, but it was taken up by several other companies, and some versions are now offered for sale to the aero clubs.

The power supply voltage of the Efan motor was equal to 300 V, we think that a VLV version would make sense to facilitate the maintenance operations of the aircraft, if it is particularly used in the aero clubs. This approach is all the more interesting as it also allows the search for very high specific performances thanks to the properties of the winding with only one solid bar per slot. The weight of the motor is, of course, one of the first sizing criteria.

Figure 20.
High frequency electric motor prototype. (a) Wound stator. (b) Rotor assembly.

Dimensions	
Stator outer diameter	137 mm
Stator inner diameter	120mm
Magnetic airgap length	1 mm
Stator stack length	92 mm
Winding bar dimensions (hxw)	3x5 mm
Slot dimensions (hxw)	4x6 mm
Materials	
Stator corepack	Iron-Cobalt, 0,2 mm
Magnets	N35EH
Electrical parameters	
Pole / slot number	40 / 36
Phase rated current	400 A RMS
Phase resistance (AC, K_{AC} = 1,44), 20 °C - 100 °C	1,85 mΩ - 2,44 mΩ
Torque coefficient kt	0,125 Nm/A
Total weight (including mechanics)	6 kg
Nominal torque-to-weight ratio	8.3 Nm/kg
Nominal power-to-weight ratio	4,3 kW/kg
Joule losses (at 100 °C)	1200 W
Iron losses + mechanical losses	400 W
Efficiency	94%
Cooling method	Natural convection

Table 5.
Characteristics of the electric aircraft motor.

To maximise the power-to-weight ratio, we have designed an electric motor operating at high frequency. The winding structure is special [1, 4, 5, 14], where the phases are arranged in six separate sectors, the electrical phase shift is ensured by introducing an intermediate irregular tooth, as illustrated in **Figures 4, 19** and **20**. This winding design allows, on the one hand, to keep a limited number of slots (36 slots), despite the large number of poles (40 poles), and, on the other hand, to avoid the end-windings overlaps, resulting in very short overhangs.

The simplified specifications are as follows:

- Maximum power: 26 kW
- Maximum speed: 5000 rpm
- Power supply voltage: 80 VDC
- Weight: less than 7 kg
- Efficiency: greater than 92%

The **Table 5** shows the main characteristics of the electric motor.

The structure with large number of poles allows to obtain high specific power, more than 4 kW/kg. The VLV winding contributes to this level of performance without compromising the efficiency. The additional loss coefficient, K_{AC}, remains moderate despite operating at a frequency of 1666 Hz. As the motor is placed behind the propulsion propeller, the 1600Wof total losses will be easily evacuated.

6. High power vehicles

When the required power of the vehicle motorisation exceeds the threshold of 30 kW (approximate), it becomes difficult, if not impossible, to supply the motor with a single controller because the phase currents become prohibitive at VLV. The two examples discussed in this paragraph show how to solve this problem using power partitioning.

6.1 Sporty electric vehicle

The first considered case of high power motorisation is that of a rally type sporty vehicle (**Figure 21**).

Figure 21.
Sporty full electric vehicle.

The simplified specifications of the motor are as follows:

- Maximum power: 100 kW
- Maximum speed: 5000 t/mn
- Power supply voltage: 100 VDC

In order to divide the power supplied to the motor, the winding was designed based on the technique described earlier in **Figure 15**, and is split into two electrically isolated stars, as depicted in the following **Figure 22**; each half-winding being fed by a dedicated controller and delivering half of the total required power.

Table 6 summarises all the main characteristics of the electric motor. In this case, we are using the solid bar configuration corresponding to case 3 in **Table 2**.

The losses at simultaneously maximum power and maximum speed are too high, more than 7 kW, particularly due to a high K_{AC} coefficient, but this is only a transient regime occurring during the acceleration phase. Again, here the steady-state thermal behaviour also depends on the nature of the track which cannot be defined a priori, but in all cases the efficiency is high and greater than 95%. However, at low speed acceleration, the copper losses are halved at constant current because the K_{AC} coefficient tends towards 1, the efficiency, therefore, remains high over a wide speed range. The partition of the power on multiple converters makes it possible to reduce the phase current to 650 A during the transient regime. The bar winding has allowed the design of a very compact motor reaching high power density (4 kW / kg in transient regime).

6.2 Utility vehicle

The second example of power partitioning is that of an utility vehicle, an electric tractor for winegrowers (**Figure 23**).

This tractor is equipped with four electrified wheels fully independent. The topology of the motors is very similar to that described in section 4. The solid bars configuration corresponds to line 4 of **Tables 1** and **2**. The four electric motors drive the wheels via a gearbox with a reduction ratio of 1/40.

The simplified specifications of the motors are as follows:

- Maximum power: 40 kW
- Rated power: 5 kW

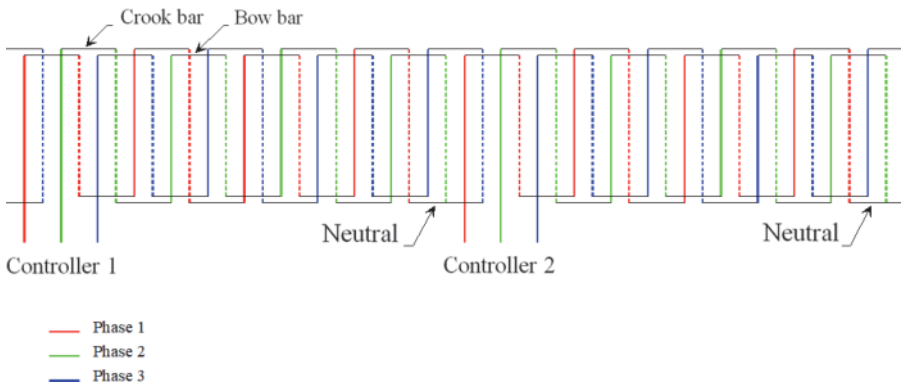

Figure 22.
Dual stars winding layout.

Dimensions	
Stator outer diameter	204 mm
Stator inner diameter	156 mm
Magnetic airgap length	2 mm
Magnet height	5 mm
Stator stack length	175 mm
Winding bar dimensions (hxw)	8x4 mm
Slot dimensions (hxw)	9x5 mm
Materials	
Stator corepack	M270-35A
Magnets	N35UH
Electrical parameters	
Pole number	16
Slot number	48
Phase rated current	650 A RMS
Phase resistance (AC, KAC = 2,39 - 2 x 3 phase), 20 °C - 100 °C	1,85 mΩ - 2,4 mΩ
Torque coefficient kt	0,46 Nm/A
Total weight (including mechanics)	40 kg
Nominal torque-to-weight ratio	7,5 Nm/kg
Joule losses (at 100 °C)	6000 W
Iron losses + mechanical losses	1400 W
Efficiency	95%
Cooling method	Natural convection

Table 6.
Characteristics of the sporty vehicle electric motor.

Figure 23.
Electric tractor.

- Maximum speed: 4000 rpm
- Nominal speed: 1000 rpm
- Power supply voltage: 80 VDC

The nominal operating condition of the electric tractor corresponds to the ploughing phase, where the displacement speed is low and the total required mechanical power does not exceed 20 kW. The tractive force applied on the plough is approximately 16 kN. The sizing was carried out based on the tractor behaviour with a conventional thermal engine.

The power partition, via the use of four electric motors, enables to have a significant power available for the transient mode, approximately 160 kW, thanks to the capacity of over-torque necessary for obstacles clearing and vehicle overspeed during the road trips. During the latter operating conditions, the motors are running without flux weakening. However, this high power is only used very rarely, and only temporarily, in the case of transporting heavy loads on steeply sloping roads.

The efficiency of each electric motor at the nominal conditions, at low speed and at an output torque of 50 Nm per motor, is about 95% and this because the copper losses in the 24 mm^2 solid bars are very low due to the very low electrical frequency (133 Hz).

7. Conclusion

According to the various examples discussed in this chapter, it can be seen that it is possible to design an electric vehicle drive train operating at very low voltage (battery voltage below 120 VDC) and over a wide power range (up to 100 kW). An original, compact and high efficiency motorisation solution using a solid bar winding has been presented. In all the cases, the sizing constraints of the motor controller have been taken into account.

Main symbols and abbreviations

AC	alternating current, alternating voltage
DC	direct current, direct voltage
δ	skin depth in AC mode
EMAG	Electromagnetic
EMC	Electromagnetic Compatibility
h_{bar}	solid bar height
h_{enc}	slot height
IGBT	Insulated Gate Bipolar Transistor
J	current density
k_{AC}	additional loss coefficient AC / DC
MOSFET	Metal Oxide Semiconductor Field Effect Transistor
P_{AC}	Joule AC losses in conductors
P_{DC}	Joule DC losses in conductors
PCB	Printed Circuit Board
R_{dson}	MOSFET drain source electrical resistance
R_{th}	heat sink thermal resistance
σ	copper fill factor
t_{bar}	solid bar width
t_{enc}	slot width
V_{DS}	MOSFET drain source voltage
VLV	Very Low Voltage

Author details

Daniel Matt[1]*, Nadhem Boubaker[2], Mourad Aitakkache[1], Philippe Enrici[1], Jean-Jacques Huselstein[1] and Thierry Martire[1]

1 University of Montpellier, Montpellier, France

2 Safran Electrical and Power, Pitstone, UK

*Address all correspondence to: daniel.matt@umontpellier.fr

IntechOpen

References

[1] Boubaker N. Study of atypical losses in high performance permanent-magnet synchronous machines for aircraft applications [thesis]. University of Montpellier; 2016.

[2] Enrici Ph, Boubaker N, Matt D. Bar Winding for the Low-Voltage Motorization of an Electric Tractor. In: Proceedings of the International Conference on Electrical Machines (ICEM); 23-26 August 2020; Gothenburg. Sweden: IEEE; 2005. p. 1711-1717.

[3] Matt D, Boubaker N. Very Low Voltage and High Efficiency Motorisation for Electric Vehicles, "Emerging Electric Machines – Advances, Perspectives and Applications", INTECH ed., ISBN 978-1-83968-732-7

[4] Lorenzo P, Matt D, Gimeno A, Boubaker N. Contribution on AC bar windings losses reduction for a high frequency and high performance machine for aeronautical application. International Symposium on Electromagnetic Fields in Mechatronics, Electrical and Electronic Engineering (ISEF); 29-31 August 2019; Nancy. France: IEEE; 2020. DOI 10.1109/ISEF45929.2019.9097026

[5] Boubaker N, Matt D, Nierlich F. A stator winding arrangement. Patent #WO2020208425A1.

[6] Levasseur A. Nouvelles formules, valables à toutes les fréquences, pour le calcul. Journal de Physique et le Radium. 1930.

[7] Liwschitz M. Calcul des machines électriques. SPES; 1967.

[8] Daou H. Méthodologie de conception numérique d'un module de puissance dédié à l'automobile en vue de l'optimisation des surtensions, des pertes et des émissions conduites, PhD thesis from the University of Paris-Saclay, 2017.

[9] Wolfgang E. Examples for failures in power electronics systems. ECPE Tutorial Reliability of Power Electronic Systems, April 2007.

[10] Yang S, Bryant A, Mawby P, Xiang D, Ran L, Tavner P. An industry based survey of reliability in power electronic converters. IEEE Transactions on Industry Applications, Vol. 47, no 3, May/June 2011. P 1441-1451.

[11] O'keefe M, Vlahinos A. Impacts of cooling technology on solder fatigue for power modules in electric traction drive vehicles. 5th IEEE Veh. Power Propuls. Conf. VPPC '09, p. 1182-1188, 2009.

[12] Liang Z. Status and trend of automotive power packaging. Int. Symp. Power Semicond. Devices ICs, vol. 1, p. 325-331, 2012.

[13] Olszewski M. Evaluation of the 2008 LEXUS LS 600H "Hybrid Synergy Drive System". US Department of Energy, Washington DC, 2009.

[14] Boubaker N, Matt D, Enrici Ph, Nierlich F, Durand G. Measurements of Iron Loss in PMSM Stator Cores Based on CoFe and SiFe Lamination Sheets and Stemmed From Different Manufacturing Processes. IEEE Transactions on Magnetics, 2018; DOI: 10.1109/TMAG.2018.2877995